4-18-2017

Mermin Inequalities for Perfect Correlations in Many-Qutrit Systems

Jay Lawrence
Dartmouth College

Mermin inequalities for perfect correlations in many-qutrit systems

Jay Lawrence

Department of Physics and Astronomy,

Dartmouth College, Hanover, NH 03755, USA and

The James Franck Institute, University of Chicago, Chicago, IL 60637

(Dated: revised July 31, 2017)

Abstract

The existence of GHZ contradictions in many-qutrit systems was a long-standing theoretical question until it's (affirmative) resolution in 2013. To enable experimental tests, we derive Mermin inequalities from concurrent observable sets identified in those proofs. These employ a weighted sum of observables, called $\mathcal{M}$, in which every term has the chosen GHZ state as an eigenstate with eigenvalue unity. The quantum prediction for $\mathcal{M}$ is then just the number of concurrent observables, and this grows asymptotically as $2^N/3$ as the number of qutrits $N \to \infty$. The maximum classical value falls short for every $N \geq 3$, so that the quantum to classical ratio (starting at 1.5 when $N = 3$), diverges exponentially ($\sim 1.064^N$) as $N \to \infty$, where the system is in a Schrödinger cat-like superposition of three macroscopically distinct states.

PACS numbers: 03.67-a, 03.65.Ta, 03.65.Ud

I. INTRODUCTION

Bell's inequality [1] shows that no local hidden variable theory (HV) can duplicate the quantum predictions for the correlations of two distant spin-1/2 particles (in Bohm's model [2] of the original EPR scenario [3]). Specifically, the maximum quantum value of a certain correlation operator exceeds the maximum value allowed by HVs, with both quantum and HV predictions being probabilistic. It was not known for another quarter century (1964-1989) whether a stronger theorem existed, allowing for a definite (non-probabilistic) quantum prediction, until Greenberger, Horne, and Zeilinger (GHZ) [4] found one for a system of three spin-1/2 particles [5]. Here, the product of three spin projections measured at distant points is predicted to take a single definite value, despite the randomness of the local measured values. The definiteness of the quantum prediction elevates HVs to the status of EPR elements of reality, since knowledge of local observables at two distant points allows prediction "with certainty" of that at the third point. On a practical level, this definiteness is essential in quantum information protocols such as quantum error correction [6] and quantum secret sharing [7].

In 1990, Mermin [8] generalized the GHZ proof and supplied a Bell inequality for all $N \geq 3$ based on the perfect correlations predicted by quantum mechanics. This was done to enable future experimental tests of GHZ contradictions by accounting for inevitable uncertainty in actual measurements, despite their absence in principle. Experimental tests have indeed made use of such inequalities (now called Mermin inequalities) to demonstrate GHZ contradictions with a probability of many standard deviations. The first such test [9] came a decade later; a recent test [10] describes the current state of the art.

Extensions of Mermin's work within qubit sytems include GHZ contradictions based on stabilizer groups of particular error-correcting codes [11], and Mermin-like inequalities based on stabilizers for all graph states of $N \leq 6$ [12]. In the latter work (2008), Cabello et. al. defined a Mermin inequality as a Bell inequality for which (I) the Bell operator is a sum of stabilizing operators that represent the perfect correlations in their simultaneous eigenstate, and (II) the ratio of quantum to maximum classical value is a maximum for that state. We shall propose a modest extension below.

Equally interesting for us are the extensions to higher dimensions (d), which differ for even and odd cases. Extensions to higher *even* dimensions include GHZ contradictions and

Kochen-Specker identities [13, 14] for *odd* $N > d$ (2002), then GHZ contradictions for odd $N < d$ [25] (2006), and more recently (2013), GHZ contradictions and corresponding Mermin inequalities [16] for systems of *all* $N \geq 4$ (with even d), using GHZ-type graph states.

Regarding *odd dimensions*, Bell inequalities have been derived for systems of three [17] or more [18] qutrits, as well as for higher odd d [19]. However, these are not Mermin inequalities; their quantum predictions are not definite, so they do not establish an underlying GHZ contradiction. In fact, prior to (2013), it was not known whether a GHZ contradiction existed for any odd d. It is now known that they do exist [20, 21], and their discovery led to the completion of the program to establish GHZ contradictions (theoretically) for all $N \geq 3$ for every $d \geq 2$ [21]. However, it is also known that these odd-d contradictions cannot be based on stabilizer sets [22], as is typical in even dimensions – a conclusion drawn from studies of the discrete Wigner function for odd dimensions [23, 24].

The newly discovered GHZ contradictions in odd-d systems [20, 21] are based on concurrent observables [25] - observables that are not compatible but have a common eigenstate. These are not the stabilizers usually associated with graph states, both because they lack compatibility and because local measurement bases are not exclusively those of the generalized Pauli operators. However, these aspects do not comprise experimental testing, for which the essential distinction between Bell and Mermin inequalities is the definiteness of the quantum predictions. Thus, it seems appropriate to broaden the definition of a Mermin inequality by deleting the word "stabilizing" from statement I (paragraph 3) above.

The purpose of this article is to construct Mermin inequalities, in this broader sense, for systems of $N \geq 3$ qutrits, from sets of concurrent observables that share a GHZ eigenstate, violations of which would establish the perfect correlations of GHZ contradictions. Entangled multiple-qutrit states are now being investigated experimentally [26], and such inequalities will enable experimental tests of GHZ contradictions. In the next section we present results for all $N \geq 4$; the exceptional case of $N = 3$ is presented in Sec. III, and in Sec. IV we discuss conclusions and open questions.

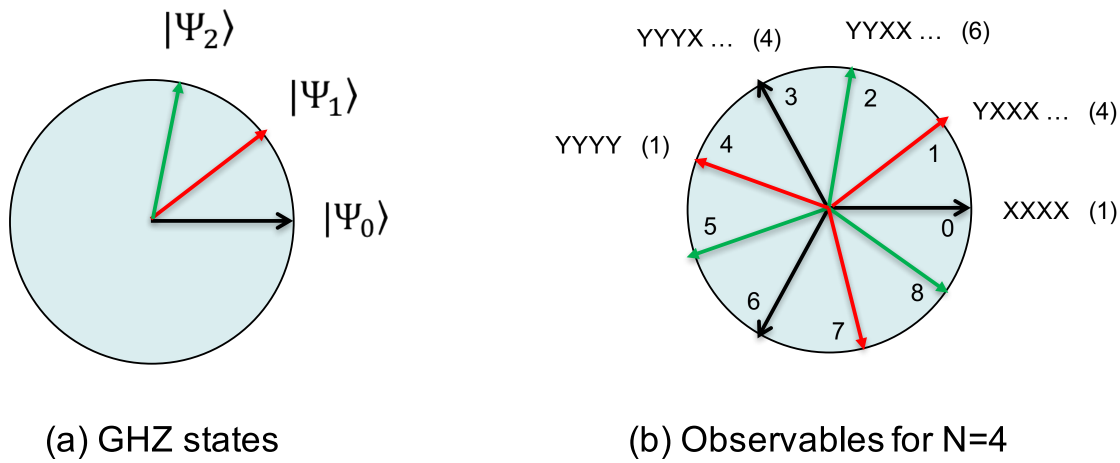

FIG. 1: (a) GHZ states (Eq. 1), and (b) tensor product observables for N=4. Parentheses denote the number of permutations. Black arrows define the concurrent subset (of five observables) whose joint eigenstate is $|\Psi_0\rangle$.

II. MERMIN INEQUALITIES FOR $N \geq 4$

It will be useful to consider three choices of GHZ state that differ by relative phases of components,

$$|\Psi_k\rangle = \frac{1}{\sqrt{3}}\big(|00...0\rangle + \alpha^k|11...1\rangle + \alpha^{2k}|22...2\rangle\big), \qquad (k = 0, 1, 2), \tag{1}$$

where $\alpha = \exp(2\pi i/9)$. Envisioning the qutrits as spin-1 particles, Fig. 1a illustrates that $|\Psi_1\rangle$ is obtained from $|\Psi_0\rangle$ (and $|\Psi_2\rangle$ from $|\Psi_1\rangle$) by rotations of $2\pi/9 = 40^o$. Such "rotations" refer to any combination of individual qutrit rotations about their respective $\hat{z}$ axes, by increments adding up to $2\pi/9$. A defining symmetry of GHZ states is that the rotated state is independent of the distribution of these increments among qutrits [21].

The corresponding observable sets of which $|\Psi_k\rangle$ are joint eigenstates are also related by compound rotations. The starting point is the basic observable,

$$\mathbf{X} \equiv X^{\otimes N} = X_1...X_N, \tag{2}$$

where each factor X_i is the qutrit Pauli matrix ($X = \sum_{n=0}^{2} |n+1\rangle\langle n|$) that defines the first local measurement basis. The second local basis (Y_i) is defined by a $2\pi/9$ rotation of X_i,

$$Y \equiv Z^{1/3} X Z^{-1/3} = \sum_{n=0}^{2} |n+1\rangle \alpha^{(1-3\delta_{n,2})}\langle n|, \qquad \text{where} \quad Z = \sum_{n=0}^{2} |n\rangle \omega^n \langle n|. \tag{3}$$

Compound rotations of the operator $\mathbf{X}$ (Eq. 2) through $2\pi k/9$ generate tensor products in which k factors of Y are distributed in all possible ways, $\binom{k}{N}$, among $N-k$ factors of X. These operators appear at points $k = 0, ..., 8$ in Fig. 1b.

Clearly, $|\Psi_0\rangle$ is an eigenstate of $\mathbf{X}$ with eigenvalue 1. Rotational covariance of operators and states [21] means that $|\Psi_1\rangle$ is an eigenstate of all operators at the point 1, and $|\Psi_2\rangle$ of all operators at point 2 - in all cases with eigenvalue 1. Points 3 and beyond are then governed by the periodicity property [21]: Any rotation of an operator through $2\pi/3$ (*eg*, from 0 to 3) preserves its eigenstates, but multiplies its eigenvalues by ω. Therefore, $|\Psi_0\rangle$ is a joint eigenstate of operators at points 0, 3, and 6 (black arrows in Fig. 1); $|\Psi_1\rangle$ of operators at 1, 4, and 7 (red arrows); and $|\Psi_2\rangle$ of operators at 2, 5, and 8 (green arrows). In each case, the eigenvalues are 1, ω, and ω^2, respectively. We shall refer to equilateral triangles (0,1,2) defined by each set of arrows, with concurrent operators at its vertices. (Not all vertices are occupied when $N < 8$.)

The case of $N = 3$ is special because a third local measurement basis is required for GHZ contradictions. Hence we defer that case and proceed here with $N = 4$, which is the simplest case. Choosing the state $|\Psi_1\rangle$, red arrows in Fig. 1b identify the concurrent subset of five observables – the four cyclic permutations of $YXXX$, each with eigenvalue 1, and $YYYY$, with eigenvalue ω. These observables produce a GHZ contradiction [21]. For the corresponding inequality, we define the Mermin operator,

$$\mathcal{M}_1 = (YXXX + \text{permutations}) + \omega^2 YYYY, \tag{4}$$

of which $|\Psi_1\rangle$ is clearly an eigenstate with eigenvalue $\mathcal{M}_Q = 5$. This "quantum value" is to be compared with the maximum HV value. The *general* HV value, which we call $v(\mathcal{M}_1)$, depends on the values (1, ω, or ω^2) assigned to each of the local factors [thence called $v(X_i)$ and $v(Y_i)$], which must be the same in each of the five tensor products. It is easy to see that $|v(\mathcal{M}_1)|$ depends only on the local ratios,

$$R_i = v(Y_i)/v(X_i), \tag{5}$$

where, hiding an irrelevant overall phase factor, $v(\mathbf{X})$, it is simply

$$|v(\mathcal{M}_0)| = |R_1 + R_2 + R_3 + R_4 + \omega^2 R_1 R_2 R_3 R_4|. \tag{6}$$

It is easy to verify by explicit calculations that the maximum value, $\mathcal{M}_{HVM}$, is obtained with either of two HV models: (i) uniform R_i (*eg*, $R_i = 1$), and (ii) a single departure from uniformity (*eg*, $R_1 = \omega$ and all others = 1). This maximum value is

$$\mathcal{M}_{HVM} = |4 + \omega^2| = \sqrt{13} \approx 3.61, \tag{7}$$

so that the ratio of quantum to maximum HV values is

$$\mathcal{A} = \mathcal{M}_Q / \mathcal{M}_{HVM} = 5/\sqrt{13} \approx 1.39. \tag{8}$$

Clearly the alternative choice, $|\Psi_0\rangle$, together with operators at points 0 and 3, would result in the same values of $\mathcal{M}_Q$ and $\mathcal{M}_{HVM}$, while the choice $|\Psi_2\rangle$, with operators only at point 2, would result in $\mathcal{M}_Q = \mathcal{M}_{HVM} = 5$, showing no GHZ contradiction. Therefore, $\mathcal{M}_0$ and $\mathcal{M}_1$ are equally valid Mermin operators, according to the definition.

For arbitrary $N > 4$, we pick a state $|\Psi_k\rangle$ and identify its candidate Mermin operator $\mathcal{M}_k$ as the sum all concurrent operators at the vertices of the corresponging triangle, with weighting factors 1, ω^2, and ω assigned to first, second, and third vertices traversed in counterclockwise order. As above, the results ($\mathcal{M}_Q$ and $\mathcal{M}_{HVM}$) depend on the choice of k, and Table I shows those choices which maximize the ratio $\mathcal{A}$ and produce Mermin operators. For even N, by symmetry, there are two such choices; for odd N, only one. The corresponding quantum eigenvalues are given by

$$M_Q = \frac{1}{3}(2^N - 1) \quad \text{(even } N\text{)}; \qquad\qquad M_Q = \frac{1}{3}(2^N - 2) \quad \text{(odd } N\text{)}; \tag{9}$$

equal to the total number of concurrent observables on the kth triangle.

The contrasting $\mathcal{M}_{HVM}$ values are maxima of $|v(\mathcal{M}_k)|$, given k on the Table, over the local ratios R_i (Eq. 5). In the following six paragraphs, we show how these are determined, including the proof of the following –

Theorem: Maximum values of $|v(\mathcal{M}_k)|$, for k values listed on Table I, are attained with uniform R_i in all cases except N = 5, 7, and 9, where the simplest nonuniform model ($R_1 = \omega$, $R_2 ... R_N = 1$) narrowly prevails.

Proof: A closed-form expression for candidate Mermin operators (valid for k = 0, 1, or 2) is [27]

$$\mathcal{M}_k = \frac{1}{3}\Big[(X + \alpha^2 Y)^N + \omega^{2k}(X + \omega\alpha^2 Y)^N + \omega^k (X + \omega^2\alpha^2 Y)^N\Big]. \tag{10}$$

To verify, one can easily see that certain powers of Y arising in the binomial expansions cancel out because $1 + \omega + \omega^2 = 0$. With $k = 0$, for example, this cancellation leaves only the powers 0, 3, 6, ..., exactly those terms residing on the vertices of the $k = 0$ triangle in

TABLE I: Quantum and maximum HV values of the N-qutrit Mermin operator, and their ratio $\mathcal{A}$, as functions of N. Listed values of k are those which maximize $\mathcal{A}$.

N	k	$\mathcal{M}_Q$	$\mathcal{M}_{HVM}$	$\mathcal{A}$
4	0,1	5	$\sqrt{13}$	1.39
5	1	10	7	1.43
6	1,2	21	$3\sqrt{19}$	1.61
7	2	42	24	1.75
8	2,0	85	$\sqrt{2269}$	1.78
9	0	170	$\sqrt{6892}$	2.05
10	0,1	341	$\sqrt{29,791}$	1.98
11	1	682	308	2.21
12	1,2	1365	$\sqrt{385,947}$	2.20
13	2	2730	1131	2.41

Fig. 1b; and similarly for $k = 1$ and 2. One can also verify that the relative vertex weighting factors are (1, ω^2, and ω), as required, once the higher powers of α have been reduced (*eg*, $\alpha^4 = \omega\alpha$, *etc.*). (Note that $\mathcal{M}_k$ appears with overall multiplying factor α^{2k}.)

The main utility of 10 is to make the R_i-dependence explicit in

$$|v(\mathcal{M}_k)| = \frac{1}{3}\left|\prod_{i=1}^{N}(1+\alpha^2 R_i)^N + \omega^{2k}\prod_{i=1}^{N}(1+\omega\alpha^2 R_i)^N + \omega^k\prod_{i=1}^{N}(1+\omega^2\alpha^2 R_i)^N\right|. \qquad (11)$$

If the R_i are uniform, then

$$\begin{aligned} |v(\mathcal{M}_k)_{unif}| &= \tfrac{1}{3}\left|(1+\alpha^2)^N + \omega^{2k}(1+\omega\alpha^2)^N + \omega^k(1+\omega^2\alpha^2)^N\right| \\ &= \tfrac{1}{3}\left|B^N \exp(2\pi N i/9) + \omega^{2k} C^N \exp(-4\pi N i/9) + \omega^k A^N \exp(-\pi N i/9)\right|, \end{aligned} \qquad (12)$$

where the individual magnitudes are labeled so that $A > B > C$:

$$\begin{aligned} A &= |1+\omega^2\alpha^2| = 2\cos\tfrac{\pi}{9} \approx 1.8794, \\ B &= |1+\alpha^2| = 2\cos\tfrac{2\pi}{9} \approx 1.5321, \\ C &= |1+\omega\alpha^2| = 2\cos\tfrac{4\pi}{9} \approx 0.3473, \end{aligned} \qquad (13)$$

and the identity $1+e^{i\theta} = \cos\frac{\theta}{2}e^{i\theta/2}$ was used. If a single R_i differs from the rest (*eg*, $R_1 = \omega$, others unity), then the effects on Eq. 12 are to permute the coefficients, $B_1 \to C_1 \to A_1 \to B_1$ and to rotate each vector in the complex plane:

$$\begin{aligned} |v(\mathcal{M}_k)_{R_1=\omega}| &= \tfrac{1}{3} \mid B^{N-1}C\exp(2\pi Ni/9)\exp(-2\pi i/3) \\ &+ \ \omega^{2k}C^{N-1}A\exp(-4\pi Ni/9)\exp(\pi i/3) + \omega^k A^{N-1}B\exp(-\pi Ni/9)\exp(\pi i/3) \mid, \end{aligned} \quad (14)$$

where the rotation angles [$(-2\pi/3)$, $(\pi/3)$, and $(\pi/3)$, respectively] are independent of which R_i is chosen to be different.

Thus, introducing the nonuniformity decreases the two largest terms while increasing only the smallest. This can produce a net gain in $|v(\mathcal{M}_k)|$ only if the rotations bring the two largest terms into closer alignment. This unlikely scenario is actually realized in the few cases, $N = 5$, 7, and 9.

To demonstrate, first consider odd N. With k values listed on Table I, it is easy to see that the three vectors comprising $v(\mathcal{M}_k)$ in either 12 or 14 are collinear for every odd $N \geq 5$. In 12, the A term is aligned opposite to the B and C terms, so that

$$|v(\mathcal{M}_k)_{unif}| = \frac{1}{3}\Big(A^N - B^N - C^N\Big). \quad (15)$$

In 14, the C-like term is aligned opposite to the others, and so

$$|v(\mathcal{M}_k)_{R_1=\omega}| = \frac{1}{3}\Big(A^{N-1}B + B^{N-1}C - C^{N-1}A\Big). \quad (16)$$

The difference, (15 - 16), is an increasing function of N with a zero at $N_o \approx 9.26$, so that $|v(\mathcal{M}_k)_{unif}|$ is the larger for all odd $N \geq 11$, while $|v(\mathcal{M}_k)_{R_1=\omega}|$ is the larger for 5, 7, and 9. We still have to rule out more complex HV models – this is done below.

Now consider even N: Again with k values listed on Table I, one can easily see that the three vectors in Eq. 12 (uniform R_i) are minimally aligned in the complex plane (angular separations are $2\pi/3$). Nonuniformity (14) shrinks the two longer vectors as above, while the induced rotations improve their alignment somewhat (to the smaller of the angular separations $\pi/3$, $\pi/3$, and $4\pi/3$), but not enough to provide a net gain in $|v(\mathcal{M}_k)|$: Keeping the two dominant terms in each of Eqs. 12 and 14, whose angular separations are $2\pi/3$ and $\pi/3$, respectively, it is easy to show formally that $|v(\mathcal{M}_k)_{unif}| - |v(\mathcal{M}_k)_{R_1=\omega}|$ is positive for all $N \geq 6$. For $N = 4$, the exact calculations described above show that both HV models realize the maximum value. Hence $|v(\mathcal{M}_k)_{unif}|$ provides the maximum for all even N.

To rule out further HV models for all even and odd $N \geq 4$: First consider the alternate single departure, ($R_1 = \omega^2$, others unity). The largest term is reduced sharply (by C/A), the next largest is increased slightly (by A/B), while the relative alignment of these two remains unchanged. So this model is ruled out trivially. Multiple departures from uniformity may be viewed as sequences of single departures in which every step has the following properties: (i) Either it reduces the two longest vectors, or it reduces the longest by more than it increases the next-longest, and (ii) beyond the first step (which results in Eq. 14), it reproduces angular separations already seen in Eq. 12 or 14. Thus it cannot increase $|v(\mathcal{M}_k)|$ beyond the larger of $|v(\mathcal{M}_k)_{unif}|$ and $|v(\mathcal{M}_k)_{R_1=\omega}|$.

This concludes the proof of the theorem stated above. To evaluate $\mathcal{M}_{HVM}$, one may simply use Eq. 15 or 16 for odd N; for even N use 12, knowing the the angular separations are $2\pi/3$ for the listed k-values. It is also instructive for smaller N to write the Mermin operator directly from Fig. 1b and evaluate at $\{R_i\}$ determined by the theorem. Table I lists the exact maxima, $\mathcal{M}_{HVM}$, which are all integers or square roots thereof, along with rounded values of $\mathcal{A}$.

The asymptotic form of $\mathcal{M}_{HVM}$ at large N is given by the dominant term in 12, namely

$$\lim_{N\to\infty} \mathcal{M}_{HVM} = \frac{1}{3}A^N \approx \frac{1}{3}1.879^N, \tag{17}$$

so that the quantum to classical ratio (Eq. 9 to 17) diverges as 1.064^N. This exponential divergence is slow compared with Mermin's ($2^{N/2}$) for qubit systems [8]; nevertheless it represents a superposition of three macroscopically distinct states.

III. THE CASE OF N = 3

This may be the most interesting case experimentally. It is singled out here because its GHZ contradictions require three local measurement bases [21, 28]. So, while we consider the same three GHZ states (1), the concurrent operator sets must now incorporate a third local basis, a natural choice being given by rotation of individual X factors through $4\pi/9$:

$$W \equiv Z^{2/3} X Z^{-2/3} = \sum_{n=0}^{2} |n+1\rangle \alpha^{(2-6\delta_{n,0})} \langle n| \tag{18}$$

(compare 3). The observables generated by rotations of XXX now include all combinations of X, Y, and W factors, and are classified in Fig. 2 according to total rotation angles,

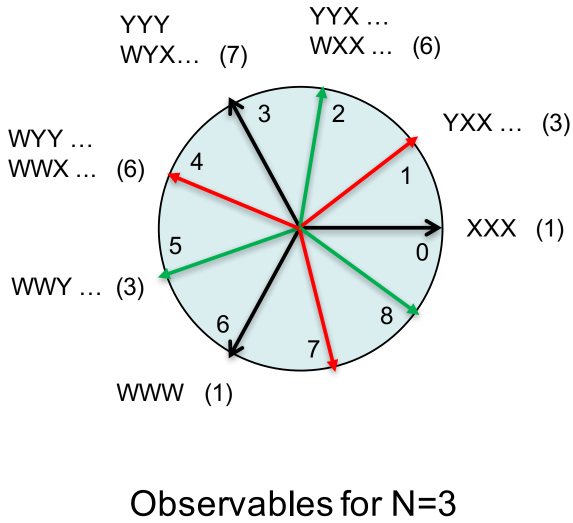

FIG. 2: Tensor product observables for N=3 form three concurrent subsets. Each produces a Mermin inequality with $\mathcal{M}_Q = 9$ and $\mathcal{M}_{HVM} = 6$.

$2\pi k/9$. Again these fall into three concurrent subsets, each associated with an equilateral triangle and its own joint eigenstate in Fig. 1a. In this case all three Mermin operators $\mathcal{M}_k$ produce the same outcome: $\mathcal{M}_Q = 9$ and $\mathcal{M}_{HVM} = 6$. Let us demonstrate with the simplest example:

$$\mathcal{M}_0 = \Big[XXX + \omega^2(YYY + XYW + XWY + YXW + WXY + YWX + WYX) + \omega WWW\Big], \tag{19}$$

with weight factors $(1, \omega^2, \omega)$ applied as required. Recall that the HV magnitude depends only on ratios, defined here as $R_i = v(X_i)/v(Y_i)$ and $S_i = v(W_i)/v(Y_i)$. So, hiding an overall irrelevant phase factor $v(YYY)$,

$$|v(\mathcal{M}_0)| = |RRR + \omega^2(111 + R1S + R1S + 1RS + SR1 + 1SR + S1R) + \omega SSS|, \tag{20}$$

where the subscripts of R_i and S_i are implied by their positions, *eg*, $R1S = R_1S_3$. Now suppose the ratios are uniform, and $R_i = S_i = 1$. Then, $|v(\mathcal{M}_0)| = |1 + 7\omega^2 + \omega| = 6$. To increase this value, one would require an HV assignment that brought the first and/or last term into equality with the seven other terms, without losing an equal number (or more) of those terms. It is easy to see that there is no such assignment.

Finally, it is interesting to note that $|v(\mathcal{M}_1)|$ and $|v(\mathcal{M}_2)|$ yield the same maximum, but both require nonuniform HV assignments, eg., ($R_1 = S_1 = \omega$ with all others unity) for the former, and, for the latter, ($S_1 = \omega$ with all others unity).

IV. CONCLUSIONS AND OPEN QUESTIONS

We have presented Mermin operators and associated inequalities for systems of $N \geq 3$ qutrits. The exceptional case of $N = 3$ requires three local measurement bases; all other cases require two. The eigenvalue of the Mermin operator (the definite quantum prediction of its measured value), is given by Eq. 9 and diverges as $2^N/3$ for large N. The maximum HV values are illustrated in Table I and reflect optimal HV assignments derived in Sec. II. These diverge as 1.879^N. The ratio of quantum to maximum HV values diverges as 1.064^N.

Ironically, the structure behind the inequalities derived here forms a close parallel with Mermin's, despite the compatibility of his observable sets as compared with the mere concurrence of those used here. This is because his Pauli tensor products and their eigenstates are related by the same rotational covariance that forms the basis of the treatment given here. It is a simple exercise to write down two alternative compatible Pauli subsets (one of which is Mermin's), and their corresponding joint GHZ eigenstates, on diagrams analogous to Fig. 1, in which the basic angular interval is $\pi/2$ rather than $2\pi/9$. Moreover, Mermin's derivation of HV maxima is based on a formula like our Eq. 10, in particular

$$\mathcal{M}_k^{d=2} = \frac{1}{2}\Big[(X + iY)^N + (-1)^k (X - iY)^N\Big], \tag{21}$$

obtained by replacing $\omega \to -1$ and $\alpha \to \exp(i\pi/4)$. The two choices $k = 0$ and 1 produce identical $\mathcal{M}_Q$ and $\mathcal{M}_{HVM}$ values, resulting in $\mathcal{A} = 2^{N/2}$ (even N), and $2^{(N-1)/2}$ (odd N).

A comparison of Eqs. 10 and 21 suggests why our exponential growth $\mathcal{A} \to 1.064^N$ is less dramatic than Mermin's. The maximum length of any factor in the HV expression for qutrits (11) is $A = |1 + \omega^2\alpha^2|^{1/2} = 2\cos\pi/9 \approx 1.8794$, no matter how HV values are assigned. The analogous length factor in the qubit case is $\sqrt{2}$. This corresponds to the different angular resolutions of vector factors in Eqs. 10 and 21, showing minimum angles in the complex plane of $\pi/9$ *vs* $\pi/4$. These differences reflect the greater freedom of qutrit HVs over qubit HVs in aiming for the quantum results.

The above comparison raises the question whether Mermin inequalities exist for systems of higher odd dimensions d, where compatible observables do not produce GHZ contradictions. It seems plausibible that a similar construction would succeed for any higher prime d, although one would expect still weaker violations of local realism for the reason given above. For higher composite dimension, a similar but more complex construction might succeed based on the smallest prime factor of d.

---

[1] J. S. Bell, *Physics* **1**, 195 (1964).

[2] D. Bohm, *Quantum Theory*, New York: Prentice Hall (1951).

[3] A. Einstein, B. Podolsky, and N. Rosen, *Phys. Rev.* **47**, 777 (1935).

[4] D.M. Greenberger, M.A. Horne, and A. Zeilinger, in *Bell's Theorem, Quantum Theory and Conceptions of the Universe*, edited by M. Kafatos (Kluwer Academic, Dordrecht, 1989), p. 69, and eprint arXiv:quant-ph/0712.0921(2007).

[5] GHZ [4] actually derived their result with four spins-1/2, mentioning in a footnote that it also holds with three.

[6] P. Shor, *Phys. Rev. A* **52**, R2493 (1995).

[7] V. Busek, A. Berthiaume, and M. Hillery, *Phys. Rev. A* **59**, 1829 (1999).

[8] N. D. Mermin, *Phys. Rev. Lett.* **65**, 1838 (1990).

[9] J.-W. Pan *et. al.*, *Nature*, **403**, 515 (2000).

[10] Z.-E. Su *et. al.*, *Phys. Rev. A* **95**, R030103 (2017).

[11] D. DiVincenzo and A. Peres , *Phys. Rev. A* **55**, 4089 (1997).

[12] A. Cabello, O. Gühne, and D. Rodríguez, *Phys. Rev. A* **77**, 062106 (2008).

[13] N.J. Cerf, S. Massar and S. Pironio, *Phys. Rev. Lett.* **89**, 080402 (2002).

[14] The connection between state-independent GHZ contradictions and Kochen-Specker identities [29] was first drawn by N. D. Mermin, *Phys. Rev. Lett.* **65**, 3373 (1990).

[15] J. Lee, S.-W. Lee, and M.S. Kim, *Phys. Rev. A* **73**, 032316 (2006).

[16] W. Tang, S. Yu, and C.H. Oh, *Phys. Rev. Lett.* **110**, 100403 (2013).

[17] A. Acin et. al., *Phys. Rev. Lett.* **92**, 250404 (2004).

[18] D. Alcina et. al., *Phys. Rev. A* **94**, 032102 (2016).

[19] W. Son et. al., *Phys Rev. Letters*, **96**, 060406 (2006).

[20] J. Ryu, C. Lee, M. Zukowski, and J. Lee, *Phys. Rev. A* **88**, 042101 (2013).

[21] J. Lawrence, *Phys. Rev. A* **89**, 012105 (2014).

[22] M. Howard, E. Brennan, and J. Vala, *Entropy* **15**, 2340 (2013).

[23] D. Gross, *J. Math. Phys.* **47**, 122107 (2006).

[24] V. Veitch, C. Ferrie, D. Gross, and J. Emerson, *New J. Phys.* **14**, 113011 (2012).

[25] J. Lee, S.-W. Lee, and M.S. Kim, *Phys. Rev. A* **73**, 032316 (2006).

[26] M. Malik et. al., *Nature Photonics*, **10**, 248 (2016).

[27] J. Kopper, private communication.

[28] J. Ryu et. al., *Phys. Rev. A* **89**, 024103 (2014).

[29] S. Kochen and E. P. Specker, *J. Math. Mech.* **17**, 59 (1967), and J. S. Bell, *Rev. Mod. Phys.* **38**, 447 (1966).